The logarithmic structure function law in wall-layer turbulence

By P. A. DAVIDSON[1], T. B. NICKELS[1] and P.-Å. KROGSTAD[2]

[1]Department of Engineering, Cambridge University, Cambridge CB2 1PZ, UK
[2]Department of Energy and Process Engineering, Norwegian University of Science
and Technology, N-7491 Trondheim, Norway

The k^{-1} spectral law for near-wall turbulence has received only limited experimental support, the most convincing evidence being that of Nickels *et al.* (*Phys. Rev. Lett. vol.* 95, 2005, 074501.1). The real-space analogue of this law is a logarithmic dependence on r of the streamwise longitudinal structure function. We show that, unlike the k^{-1} law, the logarithmic law is readily seen in the experimental data. We argue that this difference arises from the finite value of Reynolds number in the experiments. Reducing the Reynolds number is equivalent to restricting the range of eddy sizes which contribute to the k^{-1}, or $\ln r$, laws. While the logarithmic law is relatively insensitive to a truncation in the range of eddy sizes (it continues to hold over the relevant range of eddy sizes), it turns out that the k^{-1} law is not. This is a direct consequence of the so-called aliasing problem associated with one-dimensional spectra, whereby energy is systematically and artificially displaced to small wavenumbers.

1. Introduction

It has long been suggested that, for sufficiently large Reynolds number, there exists a k^{-1} region of the streamwise energy spectrum in boundary layers, k being the wavenumber (Perry, Henbest & Chong 1986). This region is thought to sit somewhere between Kolmogorov's $E \sim \epsilon^{2/3} k^{-5/3}$ inertial range and the large-scale contribution to the spectrum, the latter arising from eddies which scale on the boundary layer thickness, δ. (Here ϵ denotes the dissipation per unit mass.) Order of magnitude arguments show that, if this region exists, it lies close to the wall, deep within the log layer. The difficulty of measuring spectra very close to the wall at high Reynolds number Re may explain why clear experimental data in support of the k^{-1} law have remained elusive.

While this law is often derived on the basis of scaling and matching arguments, its physical content is quite simple. It rests on the hypothesis that, within the logarithmic region, there exists a hierarchy of eddy sizes, from y up to some fraction of δ, whose kinetic energy scales as u_*^2. (Here u_* is the friction velocity and y the distance from the surface.) If such a hierarchy of space-filling eddies exists, then the k^{-1} law follows immediately (see e.g. Davidson 2004). Of course, Townsend's attached-eddy hypothesis (Townsend 1976) pre-supposes just such a regime, and so some argue that the k^{-1} law is a direct consequence of this hypothesis (Perry *et al.* 1986). However, we wish to emphasize that any theory which leads to a hierarchy of space-filling eddies whose kinetic energy scales as u_*^2 will predict a k^{-1} law. (This is demonstrated in §3).
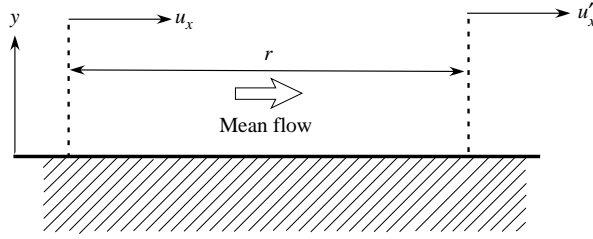
FIGURE 1. The coordinate system used in this paper.

Thus there are many competing explanations for this law, such as Högström, Hunt & Smedman (2002).

The traditional way of hunting for a k^{-1} law is to measure the one-dimensional steamwise spectrum, $\Phi_{uu}(k)$. An alternative, however, is to measure the longitudinal streamwise structure function, $\langle(\Delta u)^2\rangle(r) = \langle(u'_x - u_x)^2\rangle$. (See figure 1 for the notation used here.) Since the two are closely related (they are effectively Fourier transform pairs) the structure function should exhibit a real space analogue of the $\Phi_{uu}(k) \sim u_*^2 k^{-1}$ law, and indeed it does. The analogue is $\langle(\Delta u)^2\rangle(r) = u_*^2[A + B\ln(r/y)]$. The central thesis of this paper is that, while the k^{-1} law is relatively hard to detect in experiments, the $\ln(r/y)$ law is easier to find. The reason, we suggest, is that $\Phi_{uu}(k)$ suffers from a well-known defect in which energy is systematically and artificially displaced to low k, a phenomenon termed *aliasing* by Tennekes & Lumley (1972). While this is not a problem for $Re \to \infty$, it is a major shortcoming at the finite values of Re encountered in the laboratory, as we shall show.

2. The physical basis of the $\ln(r/y)$ law

In this section we introduce the k^{-1} law and its structure function equivalent. In particular, we show that the k^{-1} law of Perry *et al.* (1986), $\Phi_{uu}(k) \sim u_*^2 k^{-1}$, the structure function law $\langle(\Delta u)^2\rangle(r) = u_*^2[A + B\ln(r/y)]$, and Townsend's law for the streamwise velocity variance, $2u^2 = u_*^2[C + B\ln(\delta/y)]$, are all equivalent in the sense that, if any one of these three laws holds, the other two follow. In §2.1 we recall the classical explanation for these laws using the scaling arguments of Townsend and Perry. However, as noted above, any theory which predicts a hierarchy of space-filling eddies whose energy scales as u_*^2 will reproduce the k^{-1} law, and its $\ln(r/y)$ equivalent. Thus the existence of these laws does not in itself validate all of the scaling arguments used. We shall return to this point later.

2.1. *The scaling laws and physical arguments of Townsend and Perry*

We are interested in turbulent flow over a smooth wall at very high Reynolds number (though the essential ideas also apply to rough-wall boundary layers). We adopt coordinates (x, y, z) where x points in the streamwise direction and y is normal to the wall (figure 1). The second-order, longitudinal structure function, measured in the streamwise direction, is

$$\langle(\Delta u)^2\rangle(r) = \langle[u_x(x + r\hat{e}_x) - u_x(x)]^2\rangle = \langle(u'_x - u_x)^2\rangle = 2u^2(1 - f(r)), \qquad (2.1)$$

where $u^2 = \langle u_x^2\rangle = \langle u_x'^2\rangle$ is the streamwise velocity variance at x and $x + r\hat{e}_x$ respectively and $f(r) = \langle u'_x u_x\rangle/u^2$ the longitudinal correlation function. We let u_* be the friction velocity, ν the fluid viscosity, and δ the outer scale of the flow, say the boundary layer thickness or channel half-width.

Consider a level y which lies within the log layer, $v/u_* \ll y \ll \delta$. Here the dissipation per unit mass, ϵ, is of the order of $\epsilon \sim u_*^3/\kappa y$ (assuming dissipation and production are in approximate balance), κ being Kármán's constant. There are four scaling ranges for $\langle(\Delta u)^2\rangle(r)$ measured in this plane. For $r \ll y$ we have Kolmogorov scaling, where $\langle(\Delta u)^2\rangle$ is a function of ϵ, v and r. At the other extreme, $r \sim \delta \gg y$, $\langle(\Delta u)^2\rangle$ is independent of r and saturates at a value of $2u^2$. This kinetic energy is dominated by the planar sweeping motion of the large eddies whose size, s, lies in the range $y < s < \delta$. Townsend (1976) showed that the attached-eddy hypothesis predicts

$$2u^2 = u_*^2[C + B\ln(\delta/y)], \tag{2.2}$$

where C and B are constants, a law which subsequently received experimental support (Perry & Li 1990). Between these two extremes we would expect $\langle(\Delta u)^2\rangle$ to depend on ϵ, y and r, but to be independent of v and δ. To be specific, provided r is much greater than the Kolmogorov length, $\eta = (v^3/\epsilon)^{1/4} \sim (v^3\kappa y/u_*^3)^{1/4}$, yet much smaller than δ, we have $\langle(\Delta u)^2\rangle = H(r, y, \epsilon)$. Noting that $y/\eta \sim (u_*y/v)^{3/4} = (y^+)^{3/4}$, and $\epsilon \sim u_*^3/\kappa y$, we may rewrite this in the form

$$\langle(\Delta u)^2\rangle(r) = u_*^2 F(r/y), \quad (y^+)^{-3/4} \ll r/y \ll \delta/y. \tag{2.3}$$

Within this intermediate range there are two distinct subranges. For $r \ll y$ we expect local isotropy to hold (at least approximately) and so Kolmogorov's two-thirds law applies in the form $\langle(\Delta u)^2\rangle(r) = \alpha u_*^2(r/y)^{2/3}$ for $(y^+)^{-3/4} \ll r/y \ll 1$. Here α is a coefficient of order $\alpha \sim \beta/\kappa^{2/3} \sim 3.7$, where $\beta \sim 2.0$ is Kolmogorov's constant.

Conversely, for $r > y$, $\langle(\Delta u)^2\rangle$ is dominated by integral-scale eddies whose approximate size lies in the size range $y \to r$, and these have a kinetic energy of the order of u_*^2. Now $\langle(\Delta u)^2\rangle(r)$ is a measure of the contribution to $2\langle u_x^2\rangle$ of eddies of size r or less, and so $d\langle(\Delta u)^2\rangle/dr$ plays the role of an energy density. It follows that $rd\langle(\Delta u)^2\rangle/dr$ is a measure of the kinetic energy of eddies of size r (Townsend 1976), and so we expect

$$r\frac{d}{dr}\langle(\Delta u)^2\rangle \sim u_*^2, \quad y < r \ll \delta. \tag{2.4}$$

This integrates to give

$$\langle(\Delta u)^2\rangle \sim u_*^2(\ln r + D), \quad y < r \ll \delta,$$

where D is a constant of integration. Since y is the only length scale available to normalize r, we obtain

$$\langle(\Delta u)^2\rangle(r) = u_*^2[A + B\ln(r/y)], \quad y < r \ll \delta. \tag{2.5}$$

To summarize, provided that we are well-removed from the Kolmogorov scales, there are three scaling ranges (see figure 2):

$$\langle(\Delta u)^2\rangle(r) = \alpha u_*^2(r/y)^{2/3}, \quad r \ll y, \tag{2.6}$$

$$\langle(\Delta u)^2\rangle(r) = u_*^2[A + B\ln(r/y)], \quad y < r \ll \delta, \tag{2.7}$$

$$\langle(\Delta u)^2\rangle = 2u^2 = u_*^2[C + B\ln(\delta/y)], \quad r \sim \delta. \tag{2.8}$$

Note that the coefficients B in (2.7) and (2.8) are equal. This is a necessary matching condition. Physically this is because $\langle(\Delta u)^2\rangle$ acts as a filter, excluding kinetic energy from scales greater than r (Davidson 2004). The net effect of applying this filter to (2.8) is to replace δ by r. Thus we may regard (2.7) as a direct consequence of Townsend's law (2.8). Conversely, we can think of (2.8) as following directly from the structure function law.
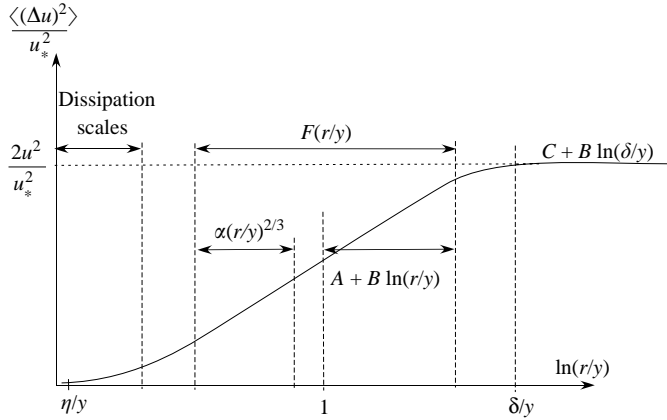
FIGURE 2. The four scaling regimes for $\langle (\Delta u)^2 \rangle$.

In this paper we are primarily concerned with the intermediate scaling (2.7). The discussion above suggests that the physical basis of this law rests on the simple hypothesis that in the subrange $y < r \ll \delta$, $\langle (\Delta u)^2 \rangle$ is dominated by eddies whose kinetic energy is of the order of u_*^2, and so (2.4) holds.

We shall see that (2.7) is well-supported by the experimental data, with $A \approx 2.04$ and $B \approx 1.83$. Note, however, that this does not imply that all of the classical scaling arguments reported here are correct. It merely confirms that there is a hierarchy of eddies whose energy scales as u_*^2. While the scaling arguments of Townsend (1976) and Perry et al. (1986) have received considerable experimental support (Perry et al. 1986; Perry & Li 1990; Marusic & Kunkel 2003) there are alternative interpretations of the evidence. For example, Högström et al. (2002) derive an equation similar to Townsend's expression (2.2) using a somewhat different line of reasoning, and since (2.7) follows directly from (2.8), via the filtering property of $\langle (\Delta u)^2 \rangle$, we could interpret support for (2.7) as support for Högström et al. (2002). In any event, for the present purposes, we are concerned only with the existence, or otherwise, of (2.7).

Finally, we note that the k^{-1} and $\ln(r)$ laws need not be restricted to boundary layers. They will appear whenever there is a hierarchy of eddies with a common velocity scale, and no externally imposed length scale. Thus the principle findings of this paper should be relevant to other flows, such as homogeneous shear flows.

2.2. The equivalence of the k^{-1} and $ln(r/y)$ laws

It is more common to formulate these arguments in spectral space, though the logic is much the same. Let $\Phi_{uu}(k)$ be the one-dimensional Fourier transform partner of $\langle u'_x u_x \rangle$:

$$\langle u'_x u_x \rangle = 2 \int_0^\infty \Phi_{uu}(k) \cos(kr) \, \mathrm{d}k. \qquad (2.9)$$

Then the spectral equivalent of (2.3) is

$$k \Phi_{uu}(k) = u_*^2 g(ky), \quad \eta \ll k^{-1} \ll \delta. \qquad (2.10)$$

Moreover, the kinetic energy of eddies of size k^{-1} is of the order of $k\Phi_{uu}(k)$, and so the hypothesis that there exists a subrange of eddies, of size $y < k^{-1} \ll \delta$, whose kinetic energy scales as u_*^2, leads to $k\Phi_{uu}(k) \sim u_*^2$. Thus, for some constant γ,

$$\Phi_{uu}(k) = \gamma u_*^2 / k, \quad y < k^{-1} \ll \delta. \qquad (2.11)$$

It is readily confirmed that, in the limit of $Re \to \infty$, the $\ln(r/y)$ and k^{-1} laws are formally equivalent, provided that $\gamma = B/4$. For example, if $\Phi_{uu}(k) = \gamma u_*^2/k$ for $y < k^{-1} < L$, but otherwise zero, then (2.9) yields $\langle (\Delta u)^2 \rangle = 4\gamma u_*^2 [\text{Ci}(r/L) - \text{Ci}(r/y) + \ln(L/y)]$, where Ci is the cosine integral. For $y \ll r \ll L$ this reduces to

$$\langle (\Delta u)^2 \rangle = 4\gamma u_*^2 [a + \ln(r/y)], \tag{2.12}$$

where $a = 0.5772$ is Euler's constant. Thus, for $Re \to \infty$, the two laws are indeed equivalent, with $B = 4\gamma$. If we wish to include the inertial range in the calculation it is more convenient to start with the structure function. For example, if $\langle (\Delta u)^2 \rangle$ is given by (2.6) for $r < y$, (2.7) for $y < r < L$, and equal to $u_*^2 [A + B \ln(L/y)]$ for $r > L$, then the inverse transform yields, for $ky \ll 1$,

$$\Phi_{uu}(k) = \frac{u_*^2}{2\pi k} [B \text{Si}(kL) + O(ky)]. \tag{2.13}$$

(Here Si is the sine integral.) It follows that, in the range $y \ll k^{-1} \ll L$,

$$\Phi_{uu}(k) = \frac{B}{4} \frac{u_*^2}{k} [1 + O(ky)]. \tag{2.14}$$

Once again we see that the $\ln(r/y)$ and k^{-1} laws are equivalent for $Re \to \infty$.

Given the similar status of the k^{-1} and $\ln(r/y)$ laws, and the marked preference for experimentalists to work with spectra rather than structure functions, it has become conventional to hunt for a k^{-1} law in $\Phi_{uu}(k)$, rather than a $\ln(r/y)$ law in $\langle (\Delta u)^2 \rangle$. However, the formal equivalence of the two laws holds only for $Re \to \infty$. For finite Re they are not equivalent, in the sense that the range over which they apply may be different, and the observed values of B and γ need not satisfy $\gamma = B/4$. Moreover, $\Phi_{uu}(k)$ is well-known to suffer from the problem of aliasing, in which energy is systematically and artificially displaced to lower k. This is particularly evident in isotropic turbulence, in which a random distribution of simple eddies of size s produces a three-dimensional spectrum of the form $E(k) \sim u^2 s(ks)^4 \exp[-(ks/2)^2]$, which peaks at around $k \sim \pi/s$, yet produces the one-dimensional spectrum $\Phi_{uu}(k) \sim u^2 s \exp[-(ks/2)^2]$, which has a maximum at $k = 0$ (see the Appendix). More generally, in isotropic turbulence,

$$\Phi_{uu}(k) = \frac{1}{2} \int_k^\infty [1 - (k/k^*)^2] \frac{E(k^*)}{k^*} \, dk^*, \tag{2.15}$$

showing that $\Phi_{uu}(k)$ is a weighted average of all the energy contained in wavenumbers k and higher (see for example Davidson 2004). It is legitimate to ask, therefore, if it makes more sense to search for a $\ln(r/y)$ law. We shall see that this is indeed the case, and that, at finite values of Re, the $\ln(r/y)$ law is evident in data where the k^{-1} law is not so clear.

We shall return to the experimental evidence shortly. First, however, we consider a model problem designed to illustrate the significant difference between the $\Phi_{uu}(k) \sim k^{-1}$ and $\langle (\Delta u)^2 \rangle \sim \ln(r/y)$ laws at finite Re.

3. The relative sensitivity of the k^{-1} and $\ln(r/y)$ laws to finite values of Re

The eddies which contribute to the $\Phi_{uu} \sim k^{-1}$ or $\langle (\Delta u)^2 \rangle \sim \ln(r/y)$ laws vary in size from $\sim y$ up to $\sim r$, where r is some fraction of δ. As $Re = u_* \delta/\nu$ is reduced, so the corresponding range of eddy sizes shrinks. It is natural to ask how this truncation in scales might affect the k^{-1} and $\ln(r/y)$ laws. In order to test this we set up a simple model problem in which we are free to vary the range of scales present in a turbulent

flow. We do not claim that this problem provides a model of the attached eddies in a boundary layer. Rather, it is designed simply to test the relative sensitivity of the k^{-1} and $\ln(r/y)$ laws to a truncation of scales. (More realistic models of a boundary layer, based on hairpin vortices, are discussed in, for example, Perry *et al.* (1986) and Perry & Li (1990).)

Our strategy is as follows. We create an artificial field of turbulence composed of space-filling eddies whose size, s, lies in the range $l \leqslant s \leqslant L$. Moreover, we suppose that the characteristic kinetic energy of these eddies is independent of size and equal to u_0^2. According to the arguments of §2, this should be sufficient to reproduce the $\Phi_{uu}(k) \sim u_0^2 k^{-1}$ and $\langle (\Delta u)^2 \rangle \sim u_0^2 \ln(r/y)$ laws, provided that $l \ll L$. (Note that the scale l in this model problem corresponds to y in the $\ln(r/y)$ law.) We then look at what happens to Φ_{uu} and $\langle (\Delta u)^2 \rangle$ as the ratio L/l is reduced. To keep the analysis simple we consider isotropic turbulence composed of a random distribution of spherical Gaussian eddies (spherical blobs of vorticity whose intensity falls off as a Gaussian), though we expect the results to be representative of eddies of other shapes, provided that they have only one characteristic length scale. Since our model problem is isotropic, whereas turbulence in a boundary layer is highly anisotropic, the results of this section must be regarded as merely suggestive. Never the less, we shall see that the predictions of our model problem are surprisingly consistent with the experimental data.

It is shown in the Appendix (see also Davidson 2004) that isotropic turbulence created from such eddies has the following energy spectrum and correlation function:

$$E(k) = \int_0^\infty \frac{\hat{E}(s)s}{12\sqrt{\pi}} (ks)^4 \exp[-(ks)^2/4]\, ds, \tag{3.1}$$

$$2u^2 f(r) = \int_0^\infty \frac{4}{3} \hat{E}(s) \exp[-(r/s)^2]\, ds. \tag{3.2}$$

Here the dummy variable s represents eddy size and $\hat{E}(s)$ is the kinetic energy density of eddies of size s. To be more specific, the kinetic energy held in eddies of size $s_1 < s < s_2$ is $\int_{s_1}^{s_2} \hat{E}(s)\, ds$. We now choose $\hat{E}(s)$ such that $\hat{E} = 0$ for $s < l$ and $s > L$, and $\hat{E}(s) = u_0^2/s$ for $l \leqslant s \leqslant L$. This ensures that the total kinetic energy of the eddies is the same from one decade of s to the next, provided of course that $l \leqslant s \leqslant L$.

Now $E(k)$ and $f(r)$ are readily calculated from (3.1) and (3.2), which in turn yields Φ_{uu} and $\langle (\Delta u) \rangle$ through, $E(k) = k^3 (d/dk)(1/k)(d/dk)\Phi_{uu}$ and $\langle (\Delta u)^2 \rangle(r) = 2u^2 - 2u^2 f(r)$. We find, after a little algebra,

$$\Phi_{uu}(k) = \frac{u_0^2}{3k}[\mathrm{erf}(kL/2) - \mathrm{erf}(kl/2)], \tag{3.3}$$

$$\langle (\Delta u)^2 \rangle = \frac{2u_0^2}{3}[\mathrm{Ein}(r^2/l^2) - \mathrm{Ein}(r^2/L^2)]. \tag{3.4}$$

where Ein is the exponential integral, $\mathrm{Ein}(x) = \int_0^x (1 - e^{-t})\, dt/t$. Now consider the case where $l \to 0$ and $L \to \infty$, while k and r remain of the order of unity. This gives

$$\Phi_{uu}^\infty(k) = \frac{u_0^2}{3k}\left[1 - \frac{kl}{\sqrt{\pi}} + O(k^2 l^2)\right] \to \frac{u_0^2}{3k}, \tag{3.5}$$

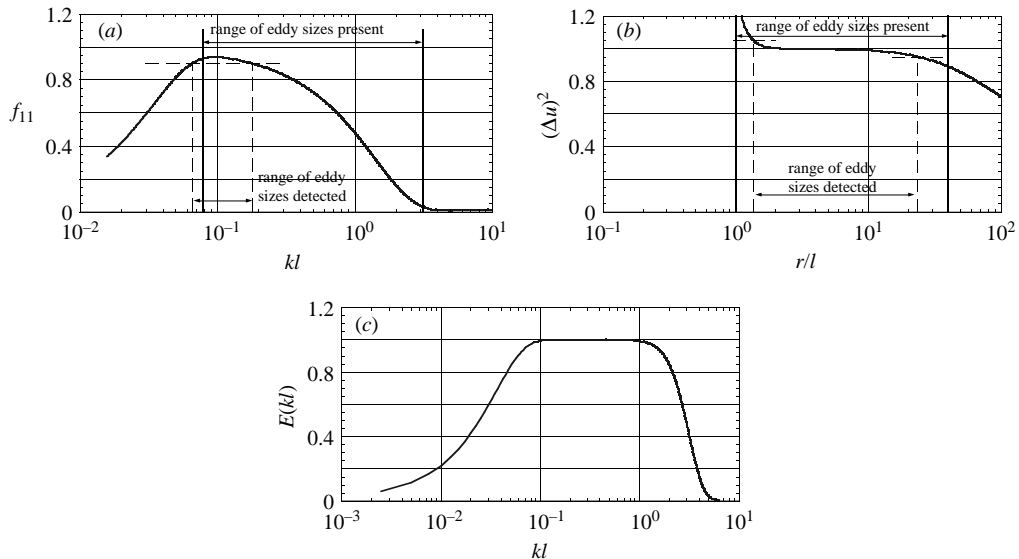$$\langle (\Delta u)^2 \rangle^\infty = \frac{4u_0^2}{3}[a/2 + \ln(r/l)], \tag{3.6}$$

FIGURE 3. (a) Φ_{uu}, (b) $\langle(\Delta u)^2\rangle$, (c) $E(k)$, all for $L/l = 40$, normalized by their value at
$L/l \to \infty$.

where a is Euler's constant. Evidently we have recovered the k^{-1} and $\ln(r/l)$ laws, as expected, with $\gamma = 1/3$ and $B = 4/3$. Note the $O(kl)$ correction to the k^{-1} law for finite l, which also appears in (2.14).

Let us now consider the effect of truncating the range of eddy sizes. We introduce the normalized functions

$$f_{11}(k) = \Phi_{uu}(k)/\Phi_{uu}^\infty(k), \qquad (3.7)$$

$$e(k) = E(k)/E^\infty(k), \qquad (3.8)$$

$$[\Delta u]^2(r) = \langle(\Delta u)^2\rangle/\langle(\Delta u)^2\rangle^\infty, \qquad (3.9)$$

whose departure from unity indicates a partial loss of the k^{-1} and $\ln(r/l)$ laws. By way of illustration, we take the case of $L/l = 40$. (The choice of 40 is motivated by the suggestion that this is typical of the range of eddies which contribute to the k^{-1} and $\ln(r/y)$ laws in our experimental data, as discussed in §4.) Figures 3(a), 3(b) and 3(c) show $f_{11}(kl)$, $[\Delta u]^2$ and $E(kl)$ for $L/l = 40$. It is immediately apparent that the deviation of $f_{11}(kl)$ from unity is much more severe than that of $[\Delta u]^2$ or $e(k)$.

Let us adopt the somewhat arbitrary convention that the $\ln(r/l)$ law is (almost) retained, in the sense that it would be discernible in an experiment, in regions where $0.95 < [\Delta u]^2 < 1.05$. (Our conclusions would be little changed if we allow for somewhat larger or smaller deviations.) In the case of f_{11} we adopt a slightly different convention, since it peaks below 1.0. Instead we say that the k^{-1} law is retained, approximately, if f_{11} lies in the range $0.9 < f_{11} < 1.0$. (Again, our conclusions would be little changed if we altered these limits.) With these somewhat *ad hoc* definitions we see that the $\ln(r/l)$ law is more or less retained in the range $1.4 < r/l < 25$, while the k^{-1} law is seen only in the very narrow region $0.07 < kl < 0.2$, rather than the expected range $(\pi/40) < kl < \pi$. Moreover, the effective prefactor in the k^{-1} law, obtained by averaging over the range $0.07 < kl < 0.2$, is $\sim 8\%$ below the ideal value of $\gamma = B/4$. We shall see that these results are typical of the experimental data.
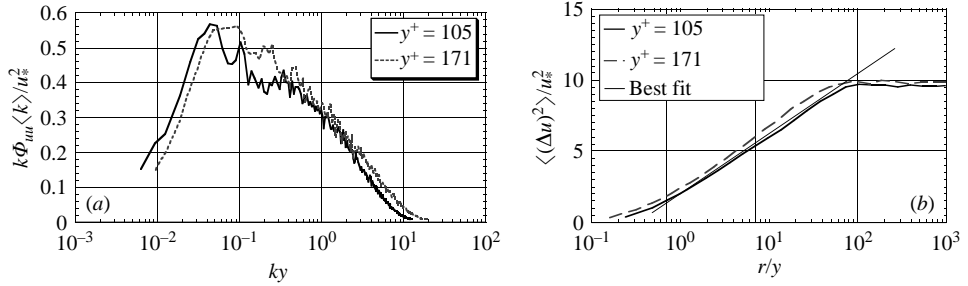
FIGURE 4. (a) $\Phi_{uu}(k)$ and (b) $\langle(\Delta u)^2\rangle$, normalized by u_* and y, for $y^+ = 105$ and 171. $Re_\theta = 12\,600$.

Figure 3 also shows the range of eddy sizes present in the turbulence. (In figure 3(a) we have used the rule of thumb that $k^{-1} \sim$ eddy size/π, which is a good approximation for spherical Gaussian eddies (Davidson 2004).) While the $\ln(r/l)$ law is retained near the centre of the range of eddy sizes, as measured on a log scale, the effective location of the k^{-1} law has been pushed to the left of figure 3(a). This is because, as shown by (2.15), one-dimensional spectra tend to systematically displace energy to larger scales, giving a distorted picture of the energy distribution. This can be confirmed by comparing f_{11} with $E(k)$. Now structure functions are themselves imperfect filters, tending to mix information about energy and enstrophy (Davidson 2004). Nevertheless, this model problem suggests that, despite the limitations of structure functions, they provide a better diagnostic tool than one-dimensional spectra.

4. The experimental data

We use here zero-pressure-gradient data obtained in two different experimental facilities. The lower-Re data were obtained in the wind tunnel at the Norwegian University of Science and Technology in Trondheim, Norway, using the facility and measurement techniques described in Skåre & Krogstad (1994). The data were taken in the same test section at zero-pressure-gradient conditions before the roof was adjusted for the adverse-pressure gradient flow reported in this paper. The higher-Re data were obtained in the high-Re boundary layer wind tunnel in Melbourne, Australia, reported in Nickels *et al.* (2005). The data apply to smooth-wall boundary layers at Reynolds numbers, based on the momentum thickness and free-stream velocity, of $Re_\theta = 12\,600$ and $Re_\theta = 37\,500$, respectively.

Let us start with the lower Reynolds number. Figures 4(a) and 4(b) show the one-dimensional spectrum and structure function data at $Re_\theta = 12\,600$ for $y^+ = 105$ and 171 ($y/\delta = 0.027$ and 0.044). Notice that there is no evidence of a k^{-1} region in figure 4(a), yet we have a clear $\ln(r)$ law in figure 4(b). The form of the $\ln(r/y)$ law is, approximately, $\langle(\Delta u)\rangle(r) = u_*^2[2.04 + 1.83\ln(r/y)]$, which is also shown on figure 4(b).

Let us now turn to the higher Reynolds number data. Again these are smooth wall data, but this time at $Re_\theta = 37\,500$. Figure 5(a) is reproduced from Nickels *et al.* (2005) and shows $\Phi_{uu}(k)$, normalized by u_* and y, in the range $100 < y^+ < 200$. Figure 5(b) shows the corresponding structure functions, again normalized by u_* and y, and obtained by Fourier transforming the data in figure 5(a).

Notice that the $\ln(r)$ law is much more evident than the corresponding k^{-1} region. Note also that the ranges over which these are seen are similar to those in our model problem, with the $\ln(r/y)$ law lying in the range $1.0 < r/y < 20$, and the k^{-1} law in
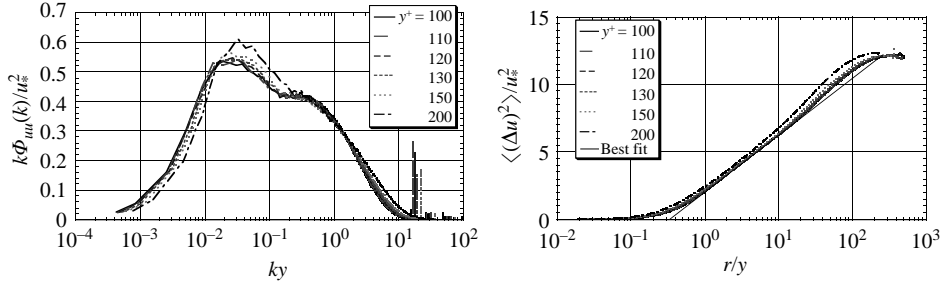
FIGURE 5. (a) $\Phi_{uu}(k)$ and (b) $\langle(\Delta u)^2\rangle$, normalized by u_* and y, in the range $100 < y^+ < 200$. $Re_\theta = 37\,500$.

the range $0.1 < ky < 0.4$. As before, the form of the $\ln(r/y)$ law is, approximately, $\langle(\Delta u)^2\rangle(r) = u_*^2[2.04 + 1.83\ln(r/y)]$, which is shown on figure 5(b) for comparison. For infinite Reynolds number this would give a value of $\gamma = B/4 = 0.458$. By comparison, the value in figure 5(a) is $\gamma \sim 0.415$, which is 9 % lower. Again, this is consistent with our model problem.

5. Conclusions

While the k^{-1} law for near-wall turbulence it difficult to see in spectra, the equivalent $\ln(r)$ law is quite evident in the equivalent structure function data. A simple model problem suggests that this arises from a well-known deficiency of one-dimensional spectra, whereby energy is systematically and artificially displaced to small wave-numbers. Certainly our model problem is consistent with the experimental data.

Appendix. Turbulence composed of Gaussian model eddies

We are interested in the kinematic properties of an artificial field of turbulence which is composed of a random distribution of eddies of given shape. This appendix is an expanded version of the analysis in Davidson (2004). Consider the vector potential $\boldsymbol{A} = \frac{1}{4}\Omega l_e^2 \exp[-2\boldsymbol{x}^2/l_e^2]\hat{\boldsymbol{e}}_z$, where l_e is the eddy size. The corresponding velocity field is a region of swirling fluid centred around the origin and of size l_e. Now suppose that we create a field of turbulence by distributing such eddies randomly yet uniformly in space. We have $\boldsymbol{A} = \frac{1}{4}\Omega l_e^2 \sum_m \exp[-2(\boldsymbol{x} - \boldsymbol{x}_m)^2/l_e^2]\hat{\boldsymbol{e}}_m$, where $\hat{\boldsymbol{e}}_m$ and $\boldsymbol{x}_m$ give the orientation and position of each eddy. (The vectors $\hat{\boldsymbol{e}}_m$ and $\boldsymbol{x}_m$ constitute a set of independent random variables.) Now consider the product of $\boldsymbol{A}(0)$ with $\boldsymbol{A}(\boldsymbol{r})$:

$$\boldsymbol{A}(0)\cdot\boldsymbol{A}(\boldsymbol{r}) = \left(\tfrac{1}{4}\Omega l_e^2\right)^2 \sum_m \exp\left[-2(\boldsymbol{x}_m)^2/l_e^2\right]\hat{\boldsymbol{e}}_m \cdot \sum_n \exp\left[-2(\boldsymbol{r} - \boldsymbol{x}_n)^2/l_e^2\right]\hat{\boldsymbol{e}}_n.$$

Since the components of $\hat{\boldsymbol{e}}_m$ and $\hat{\boldsymbol{e}}_n$ are independent random variables with zero mean we have $\langle\hat{\boldsymbol{e}}_m\cdot\hat{\boldsymbol{e}}_n\rangle = 0$ for $m \neq n$. It follows that,

$$\langle\boldsymbol{A}(0)\cdot\boldsymbol{A}(\boldsymbol{r})\rangle = \tfrac{1}{16}\Omega^2 l_e^4 \exp\left[-r^2/l_e^2\right] \sum_m \langle\exp\left[-4\boldsymbol{y}_m^2/l_e^2\right]\rangle,$$

where the quantity $\boldsymbol{y}_m = \boldsymbol{x}_m - \frac{1}{2}\boldsymbol{r}$ is a new random variable obtained from $\boldsymbol{x}_m$ by a shift of origin. Since the summation on the right is simply a coefficient which is

independent of r, we have

$$\langle \boldsymbol{A}(0) \cdot \boldsymbol{A}(\boldsymbol{r}) \rangle = \langle \boldsymbol{A} \cdot \boldsymbol{A}' \rangle = A_0^2 \exp[-r^2/l_e^2]$$

for some constant A_0. It is also readily confirmed that $\langle A_i A_j' \rangle = \frac{1}{3} \langle \boldsymbol{A} \cdot \boldsymbol{A}' \rangle \delta_{ij}$. We can now find $\langle \boldsymbol{u} \cdot \boldsymbol{u}' \rangle$ and the longitudinal correlation function, $f(r)$, from the relationships

$$\frac{1}{r^2} \frac{\partial}{\partial r} r^3 u^2 f(r) = \langle \boldsymbol{u} \cdot \boldsymbol{u}' \rangle = -\nabla^2 \langle \boldsymbol{A} \cdot \boldsymbol{A}' \rangle + \frac{\partial^2}{\partial r_i \partial r_j} \langle A_i A_j' \rangle.$$

It is readily confirmed that $f(r) = \exp[-r^2/l_e^2]$, and that the corresponding three-dimensional and one-dimensional energy spectra are

$$E(k) = \frac{\langle \boldsymbol{u}^2 \rangle l_e}{24\sqrt{\pi}} (kl_e)^4 \exp[-l_e^2 k^2/4], \quad \Phi_{uu}(k) = \frac{\langle \boldsymbol{u}^2 \rangle l_e}{6\sqrt{\pi}} \exp[-l_e^2 k^2/4].$$

Now suppose that the turbulence is composed of eddies of size l_1 (randomly but evenly distributed in space), with kinetic energy $\frac{1}{2} \langle \boldsymbol{u}_1^2 \rangle$, plus a sea of eddies of size l_2, $l_3, l_4 \ldots l_N$. In the limit where there is a continuous distribution of eddy sizes we can replace l_i by the continuous variable s and $\frac{1}{2} \langle \boldsymbol{u}_i^2 \rangle$ by the energy density $\hat{E}(s)$, which has the property

$$\frac{1}{2} \langle \boldsymbol{u}^2 \rangle = \int_0^\infty \hat{E}(s) \, \mathrm{d}s = \int_0^\infty E(k) \, \mathrm{d}k.$$

Then our expression for $E(k)$ becomes

$$E(k) = \int_0^\infty \frac{\hat{E}(s)s}{12\sqrt{\pi}} (ks)^4 \exp[-(ks)^2/4] \, \mathrm{d}s,$$

while the corresponding form for the one-dimensional spectrum is

$$\Phi_{uu}(k) = \int_0^\infty \frac{\hat{E}(s)s}{3\sqrt{\pi}} \exp[-(ks)^2/4] \, \mathrm{d}s.$$

These expressions show the relationship between the true energy density, $\hat{E}(s)$, and the spectral energy densities $E(k)$ and $\Phi_{uu}(k)$.

REFERENCES

DAVIDSON, P. A. 2004 *Turbulence, An introduction for Scientists and Engineers*. Oxford University Press.

HÖGSTRÖM, U., HUNT, J. C. R. & SMEDMAN, A. S. 2002 Theory and measurements for turbulence spectra and variance in the athmospheric surface layer. *Boundary Layer Met.* **103**, 101–124.

MARUSIC, I. & KUNKEL, G. J. 2003 Streamwise turbulence intensity formulation for flat-plate boundary layers. *Phys. Fluids* **15**, 2461–2464.

NICKELS, T. B., MARUSIC, I. HAFEZ, S. & CHONG, M. S. 2005 Evidence of the k^{-1} law in a high Reynolds number turbulent boundary layer. *Phys. Rev. Lett.* **95**, 074501.1–074501.4.

PERRY, A. E., HENBEST, S. M. & CHONG, M. S. 1986 A theoretical and experimental study of wall turbulence. *J. Fluid Mech.* **165**, 163–199.

PERRY, A. E. & LI, J. D. 1990 Experimental support for the attached eddy hypothesis in zero-pressure gradient turbulent boundary layer. *J. Fluid Mech.* **218**, 405–438.

SKÅRE, P. E. & KROGSTAD, P.-Å. 1994 Turbulent boundary layer near separation. *J. Fluid Mech.* **272**, 319–348.

TENNEKES, H. & LUMLEY, J. L. 1972 *A First Course in Turbulence*. MIT Press.

TOWNSEND, A. A. 1976 *The Structure of Turbulent Shear Flows*, 2nd Edn. Cambridge University Press.